Title: Determination of elastic stiffness coefficients of lead zirconate single crystals in the cubic phase by Brillouin light scattering

Author: J. H. Ko, Krystian Roleder, A. Bussmann-Holder

Citation style: Ko J. H., Roleder Krystian, Bussmann-Holder A. (2014). Determination of elastic stiffness coefficients of lead zirconate single crystals in the cubic phase by Brillouin light scattering. "IOP Conference Series: Materials Science and Engineering" (Vol. 54, iss. 1 (2014), art. no. 012002), doi 10.1088/1757-899X/54/1/012002

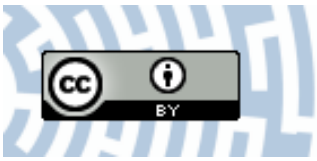

Determination of elastic stiffness coefficients of lead zirconate single crystals in the cubic phase by Brillouin light scattering

J H Ko[1], K Roleder[2] and A Bussmann-Holder[3]

[1]Department of Physics, Hallym University, 39 Hallymdaehakgil, Chuncheon, Gangwondo 200-702, Korea
[2]Institute of Physics, University of Silesia, ulica Uniwersytecka 4, PL-40-007 Katowice, Poland
[3]Max-Planck-Institut für Festkörperforschung, Heisenbergstr. 1, D-70569 Stuttgart, Germany

hwangko@hallym.ac.kr

Abstract. The temperature dependence of the three independent elastic constants of antiferroelectric lead zirconate single crystals was determined in the cubic, paraelectric phase by Brillouin light scattering spectroscopy. Two longitudinal elastic moduli of C_{11} and (C_{11}+ C_{12}+2 C_{44})/2 showed softening upon cooling toward the phase transition temperature, indicating the coupling of the acoustic waves to the polarization fluctuations of the precursor polar clusters. Among the two transverse acoustic modes, C_{44} was almost constant while (C_{11}-C_{12})/2 showed a noticeable softening in the paraelectric phase. This was attributed to the acoustic instability of lead zirconate toward the orthorhombic ground state.

1. Introduction

Lead zirconate ($PbZrO_3$, abbreviated as PZO) is one of the most representative antiferroelectric oxide materials intensively studied during the past few decades from both theoretical and experimental points of view [1]. It comprises one of the end members of famous piezoelectric $PbZr_{1-x}Ti_xO_3$ (PZT) complex perovskites, which exhibit excellent electromechanical properties at compositions near the morphotropic phase boundary. PZO undergoes an antiferroelectric phase transition at ~235°C (T_c) [2-3], below which a transient intermediate phase usually appears in a certain temperature range [4-12]. The existence of the intermediate phase is known to be sensitive to defects or stoichiometrical deviations [10]. In spite of extensive studies on this material, the exact nature of the phase transitions of PZO remains completely unsettled.

The antiferroelectric phase transition of PZO is accompanied by antiparallel shifts of the Pb atoms in the (110) plane, which coexist with the oxygen displacements undergoing antiparallel shifts within the (001) plane and along the *c* axis [9,13]. Lattice dynamic calculations also point out the coexistence of Γ point and *R* point instabilities [14]. In this respect, lattice dynamical studies are very important for better understanding of the nature of the antiferroelectric phase transition of PZO. Raman and infrared reflectivity measurements were carried out on PZO, which confirmed the existence of

[1] To whom any correspondence should be addressed.

precursor polar regions with broken symmetry in the paraelectric phase of PZO [15-16]. The measurement of the elastic stiffness coefficients (or elastic constants) is very important in relation to the interatomic potentials and their changes during the phase transition. Several theoretical calculations for elastic constants have been carried out, from which possible elastic constant values of PZO were suggested [14,17]. Recent Brillouin scattering studies showed that the predicted values from previous calculation studies are not consistent with the experimental results [18-19], demonstrating that the effective Hamiltonians used in these former calculations should be improved. In contrast, lattice dynamic calculations successfully reproduced the temperature dependence of part of the elastic constants. These clearly demonstrated that unusual lattice dynamics and large anharmonicity play an important role in the antiferroelectric phase transition of PZO [20].

In this paper, we report the details of the Brillouin scattering experiment for measuring the three independent elastic constants of PZO in its cubic phase. The detailed experimental method and results on the temperature dependence of the elastic constants will be reported. This study is in part complementary to the previous reports which include elastic data of PZO [18-20].

2. Experimental conditions

PZO single crystals were grown by using the flux growth method, i.e., from high-temperature solutions by means of spontaneous crystallization. The details of the crystal growth can be found elsewhere [18]. Several crystal plates were cut and polished to optical quality. The three orthogonal surfaces of the crystal plane were aligned along the (pseudo)cubic <100> directions. A conventional tandem 6-pass Fabry-Perot interferometer (TFP-1, JRS Co.) was used for the measurement of the Brillouin spectrum. The free spectral range was 15 GHz with a mirror spacing of 10 mm. The finesse of the interferometer was ~75. A diode-pumped solid state laser (Excelsior 532-300, SpectraPhysics) at a wavelength of 532 nm and a power of ~150 mW was used as an excitation light source. The details of the experimental setup have been described in Ref. 21.

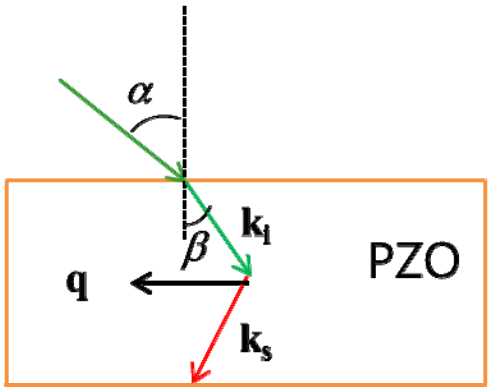

Figure 1. Forward symmetric scattering geometry.

The temperature dependence of the refractive index of PZO single crystals is usually necessary for the calculation of the elastic constants when Brillouin spectroscopy is adopted. However, a special scattering geometry, so called forward symmetric scattering geometry, may be used to obtain the elastic constants without knowing the refractive index [22]. Figure 1 shows a schematic diagram representing the forward symmetric scattering geometry. The (100) crystal plate was inserted between two cover glasses and pressed slightly by a clamp to fix it in the vertical position. Therefore, the sample is in the slightly-clamped condition rather than in the free condition. The laser beam is incident on the (100) plane with an incident angle of α ($58.7\pm0.5^{\circ}$) and is refracted into the crystal with a refraction angle of β. $\mathbf{k_i}$, $\mathbf{k_s}$ and $\mathbf{q}$ denoting the wavevectors of the incident light, scattered light and acoustic phonon, respectively. Thanks to the Snell's law, the magnitude of the phonon wavevector is

given by $4\pi \sin\alpha/\lambda$. By rotating the crystal plate in the vertical plane, the direction of the phonon wavevector **q** can be aligned along either <100> or <110> crystallographic axis in the cubic coordinates. Table 1 shows the phonon wavevector directions and elastic constants obtainable from each phonon propagation direction [23]. LA and TA modes denote the longitudinal acoustic and transverse acoustic modes, respectively.

A compact temperature controller (FTIR600, Linkam) was used for controlling the sample temperature. Temperature stability was good within ±0.1 K, but the temperature accuracy could not be assured due to the large aperture angle of the sample stage of FTIR600, which induced a substantial temperature gradient in the sample chamber. Therefore, the temperature dependence of elastic properties is shown in the relative temperature unit of T-T_c instead of the absolute temperature. The theoretically calculated density of 7.9826 g/cm^3 was used for the evaluation of the elastic stiffness coefficient based on the reported lattice constant of 4.1614 Å at 520 K [24].

Table 1. Formatting sections, subsections and subsubsections.

Wavevector	LA mode	TA mode
q || <100>	C_{11}	C_{44} (doubly degenerate)
q || <110>	$(C_{11}+ C_{12}+2 C_{44})/2$	$(C_{11}- C_{12})/2$ and/or C_{44}

3. Results and discussion

Figure 2 shows the two Brillouin spectra measured at 573 K and at two scattering geometries with different phonon propagation directions. Two clear Brillouin doublets can be seen from both scattering geometries, the high-frequency mode corresponding to the LA mode and the low-frequency one corresponding to the TA mode. The elastic constants of the LA mode appropriate to each scattering geometry can be identified without any ambiguity based on Table 1. The LA mode propagating along the <100> and <110> direction refers to C_{11} and $(C_{11}+ C_{12}+2 C_{44})/2$, respectively. The elastic constant of the TA mode at the scattering geometry of **q** || <100> is the doubly degenerate C_{44}. On the other hand, the TA mode at the scattering geometry of **q** || <110> may be either $(C_{11}- C_{12})/2$ or C_{44}. Since the temperature dependence of the TA mode at this scattering geometry is substantially different from that at the former case, we can safely identify the elastic constant of the TA mode measured at the geometry of **q** || <110> as $(C_{11}- C_{12})/2$.

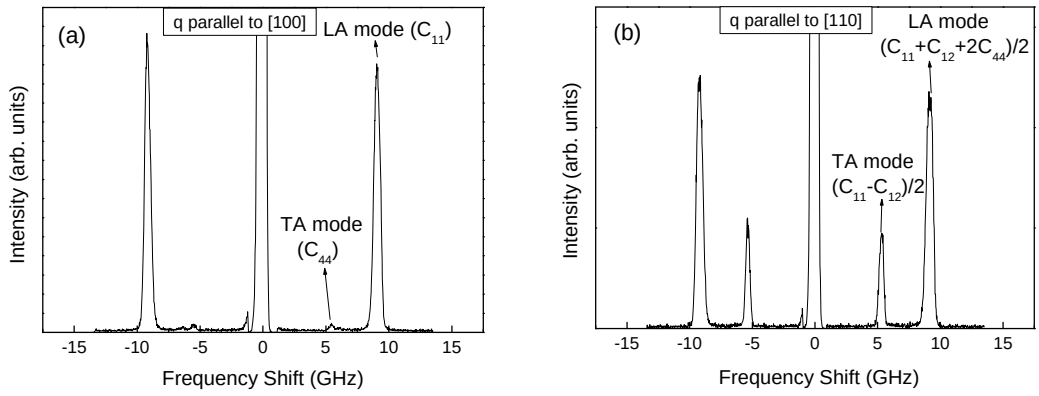

Figure 2. Brillouin spectra of PZO single crystals obtained at two different scattering geometries.

Figure 3 shows the temperature dependence of all the measured elastic constants obtained from the two scattering geometries [19]. The large experimental error bars were mostly due to the uncertainty in determining the small scattering angle (about 59°) we used in the present experiment. Table 2 shows the elastic constant values at two temperatures. The estimated error bar is approximately ±3 GPa and ±1 GPa for the LA and TA mode elastic constants, respectively.

Two longitudinal moduli, i.e., C_{11} and (C_{11}+ C_{12}+2 C_{44})/2 exhibit similar elastic softening upon cooling toward T_c, but the softening of C_{11} is more substantial. C_{11} decreases from ~212 GPa at (T_c+151) K to ~180 GPa near T_c. The values near T_c are still larger than the calculated values by first-principles studies (~151−161 GPa) in the cubic phase [14,17], suggesting that a more refined approach is necessary. The softening of the LA mode in the paraelectric phase was also confirmed from other perovskite polar oxides such as barium titanate ($BaTiO_3$) [25]. The softening of the LA mode was accompanied by the growth of the hypersonic damping as well as the appearance of a quasielastic central peaks [18,25]. These anomalous behaviors were attributed to the formation of precursor polar regions with locally broken symmetry and their electrostrictive interactions with the strains induced by acoustic waves in the paraelectric phase [26].

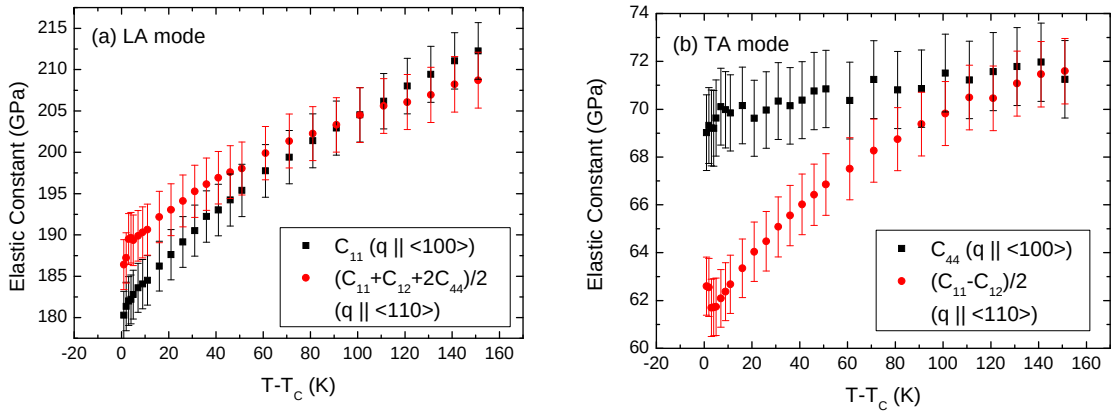

Figure 3. Temperature dependence of the elastic constants obtained from the LA and TA mode behaviors. (See Ref. [19])

The two TA modes shown in Fig. 3(b) exhibit distinct temperature dependences. C_{44} is almost constant while (C_{11}-C_{12})/2 shows a large softening in the paraelectric phase. C_{44} decreases from ~72 GPa at (T_c+151) K to ~63 GPa near T_c. This is in contrast to perovskite relaxors such as $Pb(Mg_{1/3}Nb_{2/3})O_3$ and $Pb(Mg_{1/3}Ta_{2/3})O_3$ [27], which exhibit noticeable softening of C_{44} upon cooling in the paraelectric phase. There are three symmetrized elastic constants in the cubic phase, that is, C_{11}+2C_{12}, (C_{11}-C_{12})/2 and C_{44} [28]. These three constants are related to the acoustic instabilities of the hydrostatic, tetragonal or orthorhombic, and rhombohedral deformation in sequence. The softening of C_{44}'s confirmed from relaxor ferroelectrics [27] were discussed in connection with the growth of the rhombohedral polar nano-regions in the paraelectric, nonpolar phase [29]. In contrast, the ground state of PZO is the orthorhombic phase. Therefore, it is reasonable that (C_{11}-C_{12})/2, instead of C_{44}, exhibits relatively large softening in the paraelectric phase upon cooling toward the orthorhombic phase. However, complete softening is not expected from the relevant elastic constants obtained by Brillouin light scattering because it cannot probe the zone boundary soft acoustic modes [20]. Recent lattice dynamical calculations within the polarizability model [30] showed that the temperature dependence of (C_{11}-C_{12})/2 could be well reproduced in the long-wavelength limit. Strong tendency towards an incipient polar instability was suggested from the calculated lattice dynamical properties. Another recent study based on inelastic X-ray scattering combined by Brillouin scattering suggested the Γ point ferroelectric instability is the single driving force for the antiferroelectric phase transition [19]. All

these recent studies emphasize the important role of the anharmonic optic-acoustic mode coupling in the phase transition of PZO. More accurate determination of the elastic constants and the quasielastic central peaks in both paraelectric and antiferroelectric phases of PZO is under progress in order to find out the correlation between the acoustic instabilities and the antiferroelectric phase transition of PZO.

Table 2. Elastic constants of PZO at two temperatures

Temperature	$\sim(T_c+151)$	$\sim T_c$
C_{11} (GPa)	212.3	180.3
$(C_{11}- C_{12})/2$ (GPa)	71.6	69.0
C_{44} (GPa)	71.3	62.6

4. Conclusion

The temperature dependence of elastic constants of cubic PZO single crystals was determined by Brillouin light scattering spectroscopy. C_{11} and $(C_{11}- C_{12})/2$ exhibited noticeable softening upon cooling toward the phase transition temperature. It suggests, in combination with the growing central peak [18], the existence of precursor polar regions with broken symmetry and their interactions with the acoustic waves. The softening of $(C_{11}- C_{12})/2$, instead of C_{44}, was attributed to the acoustic instability related to the orthorhombic ground state. The first measurement of the elastic constants of high-quality PZO single crystals will stimulate experimental and theoretical efforts on the understanding of the nature of the antiferroelectric phase transition of this interesting material and other related perovskite polar oxides.

Acknowledgments

This research was supported by Basic Science Research Program through the National Research Foundation of Korea (NRF) funded by the Ministry of Education, Science and Technology (2013R1A1A2006582) and by the National Center for Science (NCN) in Poland within the project 1955/B/H03/2011/40.

References

[1] Liu H and Dkhil B 2011 *Z. Kristallogr.* **226** 163
[2] Roberts S 1951 *Phys. Rev.* **83** 1078
[3] Ujma Z and Hańderek J 1975 *Phys. Status Solidi a* **28** 489
[4] Jona F, Shirane G, Mazzi F and Pepinsky R 1957 *Phys. Rev.* **105** 849
[5] Tennery V 1965 J *J. Electrochem. Soc.* **112** 1117
[6] Goulpeau L 1967 *Sov. Phys. Solid State* **8** 1970
[7] Scott B A and Burns B 1972 *J. Am. Ceram. Soc.* **55** 331
[8] Fesenko O E and Smotrakov V G 1976 *Ferroelectrics* **12** 211
[9] Whatmore R W and Glazer A M 1979 *J. Phys. C* **12** 1505
[10] Roleder K and Dec J 1989 *J. Phys.: Condens. Matter* **1** 1503
[11] Viehland D 1995 *Phys. Rev. B* **52** 778
[12] Belov A A, Jeong Y H and Kang K Y 1998 *J. Korean Phys. Soc.* **32** S299
[13] Corker D L, Glazer A M, Dec J, Roleder K and Whatmore R W 1997 *Acta Cryst. B* **53** 135
[14] Waghmare U V and Rabe K M 1997 *Ferroelectrics* **194** 135
[15] Kugel G, Jankowska-Sumara I, Roleder K and Dec J 1998 *J. Korean Phys. Soc.* **32** S581
[16] Ostapchuk T, Petzelt J, Zelezny V, Kamba S, Bovtun V, Porokhonskyy V, Pashkin A, Kuzel P,

Glinchuk M D, Bykov I P, Gorshunov B and Dressel M 2001 *J. Phys.: Condens. Matter* **13** 2677
[17] King-Smith R D and Vanderbilt D 1994 *Phys. Rev. B* **49** 5828
[18] Ko J-H, Górny M, Majchrowski A, Roleder K and Bussmann-Holder A 2013 *Phys. Rev. B* **87** 184110
[19] Tagantsev A K, Vaideeswaran K, Vakhrushev S B, Filimonov A V, Burkovsky R G, Shaganov A, Andronikova D, Rudskoy A I, Baron A Q R, Uchiyama H, Chernyshov D, Bosak A, Ujma Z, Roleder K, Majchrowski A, Ko J H and Setter N 2013 *Nature Commun.* **4** 2229
[20] Bussman-Holder A, Ko J H, Majchrowski A, Górny M and Roleder K 2013 *J. Phys.: Condens. Matter* **25** 212202
[21] Kim J H, Choi J Y, Jeong M S, Ko J H, Ahart M, Ko Y H, Kim K J 2012 *J. Korean Phys. Soc.* **60** 1419
[22] Ko J H, Jeong M S, Lee B W, Kim J H, Ko Y H, Kim K J, Kim T H, Kojima S and Ahart M 2013 *Korean J. Opt. Photon.* (in press)
[23] Vacher R and Boyer L 1972 *Phys. Rev. B* **6** 639
[24] Aoyagi S, Kuroiwa Y, Sawada A, Tanaka H, Harada J, Nishibori E, Takata M and Sakata M 2002 *J. Phys. Soc. Jpn.* **71** 2353
[25] Ko J H, Kim T H, Roleder K, Rytz D and Kojima S 2011 *Phys. Rev. B* **84** 094123
[26] Rehwald W 1973 *Adv. Phys.* **22** 721
[27] Ko J H, Kim D H and Kojima S 2008 *Phys. Rev. B* **77** 104110
[28] Cowley R A 1976 *Phys. Rev. B* **13** 4877
[29] de Mathan N, Husson E, Calvarin G, Gavarri J R, Hewat A W and Morell A 1991 *J. Phys.: Condens. Matter* **3** 8159
[30] Bussmann-Holder A and Büttner H 1992 *Nature* **360** 541